LETTERS

# Vibrational excitation through tug-of-war inelastic collisions

Stuart J. Greaves[1]*, Eckart Wrede[2], Noah T. Goldberg[3]*, Jianyang Zhang[3], Daniel J. Miller[3] & Richard N. Zare[3]

**Vibrationally inelastic scattering is a fundamental collision process that converts some of the kinetic energy of the colliding partners into vibrational excitation[1,2]. The conventional wisdom is that collisions with high impact parameters (where the partners only 'graze' each other) are forward scattered and essentially elastic, whereas collisions with low impact parameters transfer a large amount of energy into vibrations and are mainly back scattered[3]. Here we report experimental observations of exactly the opposite behaviour for the simplest and most studied of all neutral–neutral collisions: we find that the inelastic scattering process $H + D_2(v = 0, j = 0, 2) \rightarrow H + D_2(v' = 3, j' = 0, 2, 4, 6, 8)$ leads dominantly to forward scattering ($v$ and $j$ respectively refer to the vibrational and rotational quantum numbers of the $D_2$ molecule). Quasi-classical trajectory calculations show that the vibrational excitation is caused by extension, not compression, of the D–D bond through interaction with the passing H atom. However, the H–D interaction never becomes strong enough for capture of the H atom before it departs with diminished kinetic energy; that is, the inelastic scattering process is essentially a frustrated reaction in which the collision typically excites the outward-going half of the H–D–D symmetric stretch before the H–$D_2$ complex dissociates. We suggest that this 'tug of war' between H and $D_2$ is a new mechanism for vibrational excitation that should play a role in all neutral–neutral collisions where strong attraction can develop between the collision partners.**

Vibrationally inelastic scattering is usually treated by considering the repulsive part of the potential and it is assumed to happen by means of impulsive compression of one of the bonds of the collision partners. This behaviour well describes the vibrational excitation of targets with closed-shell configurations, such as $He + H_2$ (ref. 4). It has also been shown to provide an explanation for what is observed in collisions of fast H atoms with CO (ref. 5) and $CO_2$ (ref. 6). Sometimes attractive forces between the collision partners have been invoked to explain increased vibrational transfer. An example is the study of H + NO (ref. 7) in which it was suggested that vibrational excitation is enhanced by the acceleration of the incoming H atom as it passes through the well before it strikes the NO molecule and compresses the NO bond. In general, however, the attractive portion of the potential seems to play an auxiliary role in accounting for vibrational excitation when the collision energy is large in comparison with the well depth[8]. We examine the collision of fast H atoms (1.72 eV) with supersonically cooled $D_2$ molecules in which the collision energy greatly exceeds the van der Waals well depth (~3 meV) for the collinear geometry. We find that H–D attraction nevertheless plays an important role in the production of $D_2(v' = 3)$, as will be explained in what follows.

The experimental setup is virtually identical to that described in refs 9–11. A mixture of 3% HBr in $D_2$ with a typical backing pressure of 1.3 bar is introduced through a 10-Hz pulsed valve into a vacuum chamber. The reactants undergo internal and translational cooling in the supersonic expansion, and the $D_2$ is prepared almost equally in the $v = 0$, $j = 0$ and $v = 0$, $j = 2$ states. Because of symmetry (causing the preservation of ortho and para states during collision), $D_2(v = 0, j = 1, 3)$ molecules do not contribute to what is observed. Two linearly polarized, tuneable ultraviolet laser pulses ($\Delta\tau \approx 5$ ns) intersect the molecular beam at right angles. The reaction is initiated by photolysing HBr with a pulse of laser light ($\lambda \approx 209.4$ nm, $E_{pulse} \approx 300$ μJ) to produce monoenergetic H atoms with a well-defined spatial anisotropy. Single collisions with H atoms cause some of the initially cold $D_2$ molecules to become rovibrationally excited; nascent $D_2(v' = 3, j')$ is state-selectively probed via (2+1) resonance-enhanced multiphoton ionization on the Q branch lines of the (0, 3) $E,F^1\Sigma_g^+$–$X^1\Sigma_g^+$ electronic band system, where E,F refers to the double-well upper electronic state ($220.1 \leq \lambda \leq 221.9$ nm, $E_{pulse} \approx 300$ μJ). The resultant $D_2^+$ ions are formed in the extraction region of a Wiley–McLaren time-of-flight mass spectrometer and are accelerated toward a time- and position-sensitive detector whose output is analysed to determine the three-dimensional velocity of each incident particle. The PHOTOLOC (photoinitiated reaction analysed using the law of cosines) method[12] is used to map the observed laboratory-frame product speeds $|\mathbf{v}_i|$ into unique centre-of-mass scattering angles $\theta_i$, allowing the measured speed distribution to be converted into the differential cross-section $I(\theta)$.

In Fig. 1 we present the differential cross-sections for the formation of $D_2(v' = 3, j' = 0, 2, 4, 6, 8)$. In all cases a large peak in the forward-scattered direction (the same direction as the initial direction of each collision partner) is observed, although we see that a second, side-scattered peak begins to appear as $j'$ decreases, for $j' \leq 4$. This behaviour contradicts conventional wisdom for neutral–neutral inelastic scattering[3]. To seek an explanation, we carry out quasi-classical trajectory (QCT) calculations on the BKMP2 potential energy surface[13]. We note that for the $H + D_2$ reaction at a similar collision energy (2.20 eV), calculations on the BKMP2 surface using QCT and fully quantum mechanical methods have been shown to agree to a high level of accuracy[14].

The QCT methodology has been described in detail previously[15,16]. An overview of the QCT method and the potential energy surface is presented in Supplementary Figs 1–4. Five million $H + D_2(v = 0, j = 0)$ trajectories are propagated at a collision energy of 1.72 eV. The initial and final atom–diatom distances are both 6 Å and the maximum impact parameter is 1.6 Å. Trajectories are analysed on the fly and the number of times the system crosses the reaction barrier is counted (a barrier crossing event is defined as the H–D distance becoming smaller than the D–D bond length, or vice versa). Inelastic trajectories have an even number of crossings, whereas reactive trajectories have an odd number. 2,424,078 trajectories are found

[1]Laser Chemistry, Spectroscopy and Dynamics Group, School of Chemistry, University of Bristol, Bristol BS8 1TS, UK. [2]Department of Chemistry, University of Durham, Durham DH1 3LE, UK. [3]Department of Chemistry, Stanford University, Stanford, California 94305-5080, USA.
*These authors contributed equally to this work.

to be inelastically scattered, and a standard binning methodology[15] gives 842 that produce $D_2(v' = 3, j' = 0)$. Because a significant fraction of inelastic trajectories involve two or more crossings of the reaction barrier, this inelastic scattering process is closely related to reactive scattering. We therefore focus on $D_2(v' = 3, j' = 0)$ instead of $j'$ states with larger cross-sections and purer forward scattering, because of extensive existing work on the complementary reactive channel, $H + D_2 \rightarrow HD(v' = 3, j' = 0) + D$ (refs 16–25).

The reactive channel, like the inelastic channel, had been expected to proceed by means of a back-scattered direct-recoil mechanism, until a surprising forward-scattered peak in the $HD(v' = 3, j' = 0)$ differential cross-section was observed at a collision energy of 1.64 eV (ref. 17). QCT[16,17] and quantum mechanical[18,19] calculations agree that the forward-scattered peak arises from an indirect mechanism that is delayed ~25 fs relative to the direct-recoil mechanism. QCT methods, however, underestimate the intensity of the forward-scattered peak by a factor of roughly two. The reason for this discrepancy is that the forward-scattered features are influenced by interference between near-side and far-side partial waves[23,24]. As shown in Fig. 1, QCT calculations closely agree with experiments for inelastically scattered $D_2(v' = 3, j' = 4, 6, 8)$, whereas the intensity of the forward-scattered feature predicted by QCT is too small for $D_2(v' = 3, j' = 0, 2)$. This finding suggests that a similar interference effect is involved in inelastic scattering with low values of $j'$, and that a fully quantum mechanical treatment is needed to describe the observables of the system completely. Because quantum mechanical calculations for the differential cross-sections of the inelastic channel are not available in the literature, we compare in Supplementary Fig. 7 the quantum mechanical calculations of ref. 19 for reactively scattered $HD(v' = 3, j' = 0)$ with recent experiments using methods identical to those in the present work[25]. The excellent agreement supports the accuracy of both the BKMP2 potential energy surface and the present experiment on the complementary $D_2(v' = 3, j' = 0)$ inelastic scattering channel.

In Fig. 2 we present the correlation between deflection angle and impact parameter for the $D_2(v' = 3, j' = 0)$ trajectories, which agrees with conventional wisdom in that low-impact-parameter collisions are back scattered whereas high-impact-parameter collisions are forward scattered. What is surprising, however, is that high-impact-parameter collisions are effective in forming this highly vibrationally excited product. Furthermore, a correlation is found in which low-impact-parameter trajectories exhibit hard collisions exclusively leading to re-crossing of the barrier for forming HD + D, whereas high-impact-parameter collisions are more glancing in nature and show a reduced amount of re-crossing. Examination of the trajectories shows that the D–D bond is never compressed by these inelastic collisions, irrespective of whether the scattering is forward or backward. On the contrary, the D–D bond is stretched, which results from the pull of the approaching H atom on the closest D atom of $D_2$. This pull is stronger than would be expected on the basis solely of the van der Waals well depth for the equilibrium $D_2$ bond length, because the well deepens as the D–D bond lengthens (in a reactive collision, the well deepens enough to capture the H atom and form a new H–D bond).

In those collisions with high impact parameters, which dominate the process because of the weighting with impact parameter, we find that the reactants are scattered in a forward direction. At large impact parameters, the H atom approaches the $D_2$ diatom in an orientation in which the H atom's motion is nearly perpendicular to the D–D bond axis. The H atom passes through a well for the collinear configuration, but the well does not deepen sufficiently to capture the H atom. Simultaneously the H atom pulls on the nearby D atom, causing vibrational excitation of the $D_2$ diatom as the H atom escapes the shallow well with diminished kinetic energy. The H atom is not appreciably deflected from its initial direction, causing it to be forward scattered. Figure 3 illustrates this behaviour for one particular high-impact-parameter trajectory, in the form of snapshots of the H–D–D configuration as a function of time. Several representative trajectories are made available in Supplementary Videos 1–6. The lowest impact-parameter collisions forming $D_2(v' = 3, j' = 0)$ are collinear and cross the reaction barrier more than once. Some evidently go on to react and form HD + D, but others are channelled into an outward-going symmetric stretch of the H–D–D complex, which prevents the H atom from being captured by the neighbouring D atom. In this sense, these inelastic scattering events are frustrated reactive scattering events.

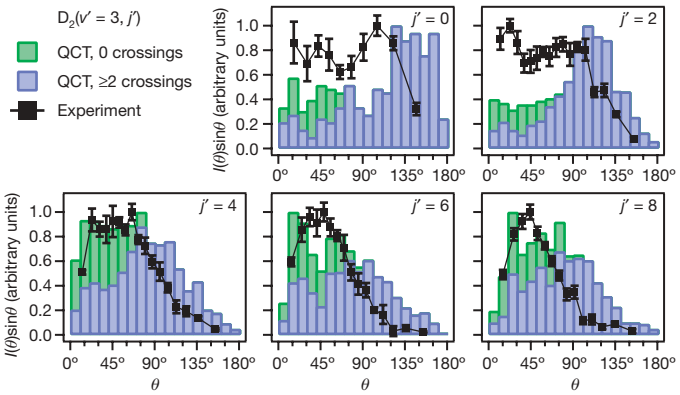


**Figure 1 | Products of inelastic H + $D_2$ collisions are mostly forward scattered.** Experimental and calculated (QCT, quasi-classical trajectory) differential cross-sections for $H + D_2(v = 0, j = 0, 2) \rightarrow H + D_2(v' = 3, j' = 0, 2, 4, 6, 8)$ inelastic collisions. Each experiment is repeated between three and seven times and the standard deviation of the replicate measurements used as an estimate of the overall error (shown in error bars). Both experiment and theory are scaled so that the peak in the differential cross-section is unity. The scattering angle $\theta$ is measured relative to the initial directions of the collision partners, so $\theta = 0^\circ$ represents perfect forward scattering (no deflection) of each collision partner. Inelastic scattering is dominated by re-crossing trajectories.

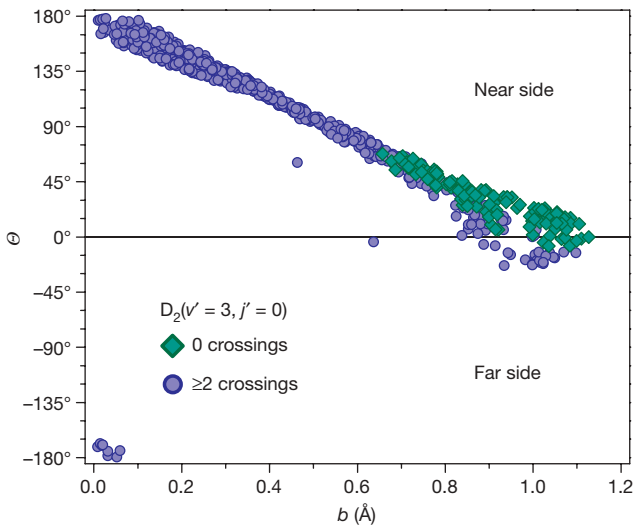


**Figure 2 | Impact parameter is linearly correlated with deflection angle.** Deflection angle $\Theta$ versus impact parameter $b$, for $D_2(v' = 3, j' = 0)$ inelastically scattered products from QCT calculations of $H + D_2(v = 0, j = 0)$ collisions at a collision energy of 1.72 eV. The strong correlation between impact parameter and scattering direction is clearly shown, with the direct trajectories having high impact parameters and being forward scattered. The deflection angle is defined as the positive scattering angle for near-side scattering (same hemisphere as the incoming H atom) and as the negative scattering angle for far-side scattering. Because of the cylindrical symmetry in the experiment, the laboratory observation is the absolute value of the deflection angle, that is, the scattering angle.

Previous work has shown that QCT overestimates the number of re-crossing trajectories (that is, more trajectories lead to inelastic scattering by crossing back into the $H + D_2$ configuration instead of forming HD + D products) in comparison with fully converged quantum mechanical calculations[22]. As shown in Figs 1 and 2, the majority of the $D_2(v' = 3, j' = 0)$ trajectories re-cross the barrier, particularly at large scattering angles. Therefore, the quantum mechanical differential cross-section would probably show less back scattering than the QCT differential cross-section, in line with the experimental result (Fig. 1). Nevertheless, the QCT calculations provide us with deep insight into the mechanisms of inelastic scattering. Because the QCT calculations and experiments are in close agreement for high-$j'$ levels of $D_2(v' = 3)$, which show one forward-scattered peak, it might be expected that the QCT calculation for $D_2(v' = 3, j' = 4)$, for example, would be more representative of the behaviour of the system. As shown in Supplementary Videos 7–10, the same tug-of-war mechanism is operative for both $D_2(v' = 3, j' = 0)$ and $D_2(v' = 3, j' = 4)$; that is, extension of the D–D bond by the incoming H atom causes vibrational excitation of the $D_2$ diatom. Again, we emphasise that $D_2(v' = 3, j' = 0)$ has both a forward- and a back-scattered peak. It might be expected that the back-scattered peak could be explained by compression of the D–D bond, but our work shows otherwise.

Forward scattering in vibrational inelastic collisions has been observed previously in ion–molecule reactions, but not to our knowledge in neutral–neutral scattering events. Vibrationally inelastic scattering of $H^+$ with $H_2$, HD and $D_2$ shows forward scattering[26], which was attributed to 'bond dilution' in which the passing proton withdraws electron density from the diatomic target, thus stretching the bond and inducing vibration. Reference 27 reported a complementary mechanism in the vibrationally inelastic scattering of $H^-$ with $H_2$, $N_2$, $O_2$ and $CO_2$, which is caused by transient charge transfer into an antibonding orbital of the target. These ion–molecule collisions are fundamentally different from what we report because there the addition or withdrawal of electron density affects the entire molecular geometry, whereas in $H + D_2$ it is only the D atom nearest to the H atom that is affected.

The conventional wisdom that neutral–neutral systems require a sudden compression of the bond must be revised. Hints of this fact were already apparent in ref. 28, which is a study of vibrational relaxation (conversion of vibration to translation and rotation) in radical–radical collisions. There it was concluded that transfer of energy out of vibration is rapidly facilitated as the intramolecular attractive force grows. We believe that this behaviour is part of the same general picture and demonstrates that tug-of-war collisions, a form of frustrated reactive collisions, can be important for open-shell collision systems having strong attractive forces arising from chemical bonding.

Tug-of-war collisions are a new mechanism for inelastic scattering that should be considered whenever it is possible for the collision system to form chemical bonds between the reactants. It must be realized, however, that such wells are not always accessible from the ground states of the collision partners, an example being H + CO (ref. 5). In the case of $H + D_2$, the well depth at the equilibrium $D_2$ bond length is quite small, but the well deepens rapidly with D–D extension. Collisions with vibrationally excited reactants would also be expected to promote this tug-of-war vibrational inelastic scattering mechanism.

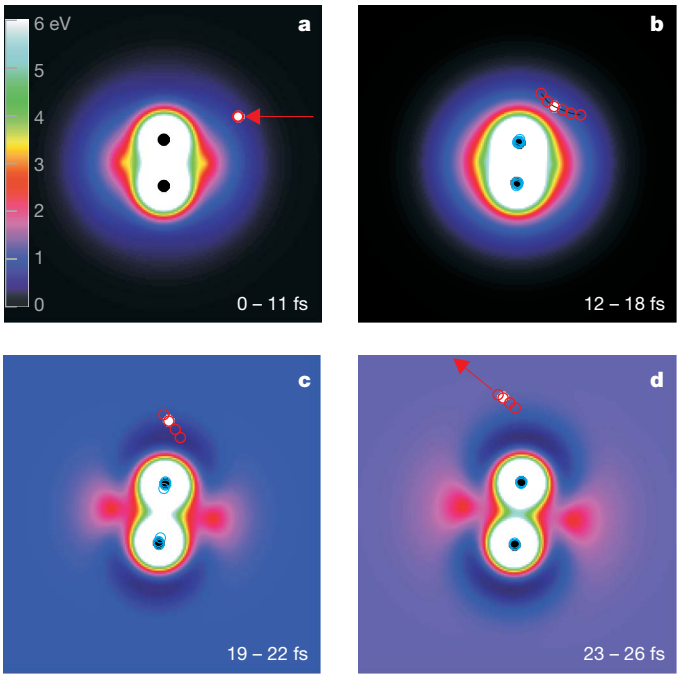


**Figure 3 | Snapshots from a representative forward-scattered trajectory.** Representative classical trajectory for a $H + D_2(v = 0, j = 0) \rightarrow H + D_2(v' = 3, j' = 0)$ inelastic collision at 1.72 eV, with a scattering angle of 40° (red arrow in **d**) with respect to the initial direction of the H atom (red arrow in **a**). The $HD_2$ potential energy surface is presented in a space-fixed frame centred at the middle of the $D_2$ bond. The 0–6-eV energy scale of the potential energy surface is shown in the colour bar: 0 eV corresponds to separation of the H atom and the $D_2$ diatom. High values of the potential energy are found perpendicular to the $D_2$ bond, owing to the conical intersection of the $HD_2$ molecule in the shape of an equilateral triangle ($D_{3h}$ geometry). The red circles represent 1.0-fs time steps of the motion of the H atom and the blue circles show the corresponding motions of the D atoms. The filled circles (white, H atom; black, D atoms) correspond to the step for which the potential energy surface is displayed. The potential energy surfaces are shown for the following $D_2$ bond lengths: 0.86 Å (11 fs, **a**), 0.72 Å (16 fs, **b**), 0.95 Å (21 fs, **c**) and 1.14 Å (25 fs, **d**). The $D_2$ bond stretches as the H atom passes through the attractive well and escapes.

**Received 20 December 2007; accepted 2 May 2008.**


1. Faubel, M. Vibrational and rotational excitation in molecular collisions. *Adv. At. Mol. Phys.* **19**, 345–394 (1983).
2. Krajnovich, D. J., Parmenter, C. S. & Catlett, D. L. Jr. State-to-state vibrational transfer in atom-molecule collisions. Beams vs. bulbs. *Chem. Rev.* **87**, 237–288 (1987).
3. Levine, R. D. *Molecular Reaction Dynamics* 376 (Cambridge Univ. Press, Cambridge, UK, 2005).
4. Miller, W. H. The semiclassical nature of atomic and molecular collisions. *Acc. Chem. Res.* **4**, 161–167 (1971).
5. McBane, G. C., Kable, S. H., Houston, P. L. & Schatz, G. C. Collisional excitation of CO by 2.3 eV H atoms. *J. Chem. Phys.* **94**, 1141–1149 (1991).
6. Kreutz, T. G. & Flynn, G. W. Analysis of translational, rotational, and vibrational energy transfer in collisions between $CO_2$ and hot hydrogen atoms: The three-dimensional "breathing" ellipsoid model. *J. Chem. Phys.* **93**, 452–465 (1990).
7. Wight, C. A., Donaldson, D. J. & Leone, S. R. A two-laser pulse-and-probe study of T-R, V energy transfer collisions of H + NO at 0.95 and 2.2 eV. *J. Chem. Phys.* **83**, 660–667 (1985).
8. Rapp, D. & Kassal, T. The theory of vibrational energy transfer between simple molecules in nonreactive collisions. *Chem. Rev.* **69**, 61–102 (1969).
9. Koszinowski, K., Goldberg, N. T., Pomerantz, A. E. & Zare, R. N. Construction and calibration of an instrument for three-dimensional ion imaging. *J. Chem. Phys.* **125**, 133503 (2006).
10. Goldberg, N. T., Koszinowski, K., Pomerantz, A. E. & Zare, R. N. Doppler-free ion imaging of hydrogen molecules produced in bimolecular reactions. *Chem. Phys. Lett.* **433**, 439–443 (2007).
11. Koszinowski, K. *et al.* Differential cross section for the $H+D_2 \rightarrow HD(v' = 1, j' = 2, 6, 10)+D$ reaction as a function of collision energy. *J. Chem. Phys.* **127**, 124315 (2007).
12. Shafer, N. E., Orr-Ewing, A. J., Simpson, W. R., Xu, H. & Zare, R. N. State-to-state differential cross sections from photoinitiated bulb reactions. *Chem. Phys. Lett.* **212**, 155–162 (1993).
13. Boothroyd, A. I., Keogh, W. J., Martin, P. G. & Peterson, M. R. A refined $H_3$ potential energy surface. *J. Chem. Phys.* **104**, 7139–7152 (1996).
14. Wrede, E. *et al.* The dynamics of the hydrogen exchange reaction at 2.20 eV collision energy: Comparison of experimental and theoretical differential cross sections. *J. Chem. Phys.* **110**, 9971–9981 (1999).
15. Greaves, S. J., Murdock, D., Wrede, E. & Althorpe, S. C. New, unexpected, and dominant mechanisms in the hydrogen exchange reaction. *J. Chem. Phys.* **128**, 164306 (2008).

16. Greaves, S. J., Murdock, D. & Wrede, E. A quasi-classical trajectory study of the time-delayed forward scattering in the hydrogen exchange reaction. *J. Chem. Phys.* **128,** 164307 (2008).
17. Fernández-Alonso, F. *et al.* Evidence for scattering resonances in the H+$D_2$ reaction. *Angew. Chem. Int. Ed.* **39,** 2748–2752 (2000).
18. Allison, T. C., Friedman, R. S., Kaufman, D. J. & Truhlar, D. G. Analysis of the resonance in H+$D_2$→HD($v'$ = 3)+D. *Chem. Phys. Lett.* **327,** 439–445 (2000).
19. Althorpe, S. C. *et al.* Observation and interpretation of a time-delayed mechanism in the hydrogen exchange reaction. *Nature* **416,** 67–70 (2002).
20. Fernández-Alonso, F. & Zare, R. N. Scattering resonances in the simplest chemical reaction. *Annu. Rev. Phys. Chem.* **53,** 67–99 (2002).
21. Ayers, J. D. *et al.* Measurement of the cross section for H+$D_2$→HD($v'$ = 3, $j'$ = 0)+D as a function of angle and energy. *J. Chem. Phys.* **119,** 4662–4670 (2003).
22. Aoiz, F. J., Bañares, L. & Herrero, V. J. The H + $H_2$ reactive system. Progress in the study of the dynamics of the simplest reaction. *Int. Rev. Phys. Chem.* **24,** 119–190 (2005).
23. Monks, P. D. D., Connor, J. N. L. & Althorpe, S. C. Theory of time-dependent reactive scattering: Cumulative time-evolving differential cross sections and nearside-farside analyses of time-dependent scattering amplitudes for the H+$D_2$→HD+D reaction. *J. Phys. Chem. A* **110,** 741–748 (2006).
24. Monks, P. D. D., Connor, J. N. L. & Althorpe, S. C. Nearside-farside and local angular momentum analyses of time-independent scattering amplitudes for the H+$D_2$($v_i$ = 0, $j_i$ = 0)→HD($v_f$ = 3, $j_f$ = 0)+D reaction. *J. Phys. Chem. A* **111,** 10302–10312 (2007).
25. Goldberg, N. T., Zhang, J., Miller, D. J. & Zare, R. N. Corroboration of theory for H+$D_2$→D+HD($v'$=3,$j'$=0) reactive scattering dynamics. *J. Phys. Chem. A*. doi: 10.1021/jp801187p (in the press).
26. Giese, C. F. & Gentry, W. R. Classical trajectory treatment of inelastic scattering in collisions of $H^+$ with $H_2$, HD, and $D_2$. *Phys. Rev. A* **10,** 2156–2173 (1974).
27. Hege, U. & Linder, F. Vibrationally inelastic scattering of $H^-$ ions from $H_2$, $N_2$, $O_2$ and $CO_2$. *Z. Phys. A* **320,** 95–104 (1985).
28. Osborn, M. K. & Smith, I. W. M. A quasiclassical trajectory study of vibrational energy transfer in collisions involving intermolecular attraction of moderate strength. *Chem. Phys.* **91,** 13–26 (1984).

**Supplementary Information** is linked to the online version of the paper at www.nature.com/nature.

**Acknowledgements** The Stanford team gratefully acknowledges support by the US National Science Foundation under grant NSF CHE 0650414. S.J.G. is supported by the EPSRC LASER Portfolio Partnership grant GR/S71750/01.

**Author Contributions** N.T.G. designed and performed the experiments with the help of J.Z. and D.J.M., analysed the experimental data, and assisted with the manuscript. S.J.G and E.W. performed quasi-classical trajectory calculations, formulated the mechanism, and prepared figures and movies. R.N.Z. wrote the manuscript. All authors discussed the results and commented on the manuscript.

**Author Information** Reprints and permissions information is available at www.nature.com/reprints. Correspondence and requests for materials should be addressed to R.N.Z. (zare@stanford.edu).